



Higgs portal dark matter and neutrino mass and mixing with a doubly charged scalar



I.M. Hierro ^{a,*}, S.F. King ^b, S. Rigolin ^a

^a Dipartimento di Fisica “G. Galilei”, Università di Padova and INFN, Sezione di Padova, Via Marzolo 8, I-35131 Padova, Italy

^b Physics and Astronomy, University of Southampton, SO17 1BJ Southampton, United Kingdom

ARTICLE INFO

Article history:

Received 22 September 2016

Received in revised form 1 March 2017

Accepted 21 March 2017

Available online 22 March 2017

Editor: J. Hisano

ABSTRACT

We consider an extension of the Standard Model involving two new scalar particles around the TeV scale: a singlet neutral scalar ϕ , to be eventually identified as the Dark Matter candidate, plus a doubly charged $SU(2)_L$ singlet scalar, S^{++} , that can be the source for the non-vanishing neutrino masses and mixings. Assuming an unbroken Z_2 symmetry in the scalar sector, under which only the additional neutral scalar ϕ is odd, we write the most general (renormalizable) scalar potential. The model may be regarded as a possible extension of the conventional Higgs portal Dark Matter scenario which also accounts for neutrino mass and mixing. This framework cannot completely explain the observed positron excess. However a softening of the discrepancy observed in conventional Higgs portal framework can be obtained, especially when the scale of new physics responsible for generating neutrino masses and lepton number violating processes is around 2 TeV.

© 2017 The Authors. Published by Elsevier B.V. This is an open access article under the CC BY license (<http://creativecommons.org/licenses/by/4.0/>). Funded by SCOAP³.

1. Introduction

The present ensemble of data from accelerators experiment seems to firmly confirm all the Standard Model (SM) ingredients to high level of accuracy, including the presence of a relatively light scalar boson (so-called “Higgs” for short) [1,2].

There are, however, few experimental indications that there should be some type of new physics beyond the SM one. The most clear indication of the need of some new kind of matter, namely the Dark Matter (DM), derives from cosmological and astrophysical observations. Assuming the WIMP ansatz, the amount of measured DM density is consistent with the existence of a weakly interacting particle with a mass around the TeV scale.

On the other side, several theoretical features of the SM still need to be elucidated, like for example the stability of the Higgs mass, the so called “hierarchy problem”, or the presence of extremely different parameters describing the masses and mixings of the SM fermions, dubbed often as the “flavour problem”.

Following the idea that the fermion mass structures could arise from a symmetry principle, flavour symmetries have been introduced, both in the context of the SM and its extensions. Many

different examples have been proposed in the literature based on a large variety of symmetries: either abelian or non-abelian, local or global, continuous or discrete [3]. Despite of all these attempts, however, it seems unlikely that the same mechanism could be responsible to generate at the same time charged and neutral fermion masses. However the unique possibility of having Majorana masses for the neutrinos, associated with the exceedingly small values of the neutrino masses, could be responsible for the differences observed in the neutrino flavour sector.

The see-saw mechanism [4], where heavy right-handed neutrinos with large Majorana masses are responsible for small effective left-handed neutrino masses, is notoriously difficult to directly test. Other mechanisms for generating neutrino masses include R-parity violating supersymmetry [5], Higgs triplet models [6–8], or loop models involving additional Higgs doublets and singlets (e.g. [9–11]). All these models can be tested experimentally (for a review of these different mechanisms see for example [12], and [13] for a very systematic study). In particular, such settings can yield very interesting connections between lepton number violating physics and collider phenomenology [14–16], especially if doubly charged scalars are involved (as in the Higgs triplet case [17,18]).

In this paper we shall focus on a particularly economical loop model of Majorana neutrino mass and mixing [19], in which the low energy effective theory involves just one extra new particle: a doubly charged EW singlet scalar S (denoting both S^{++} and its

* Corresponding author.

E-mail addresses: ignacio.hierro@pd.infn.it (I.M. Hierro), s.f.king@soton.ac.uk (S.F. King), stefano.rigolin@pd.infn.it (S. Rigolin).

antiparticle S^{--}). It is already known that such a model can lead to an interesting complementarity between low energy charged lepton flavour violation processes, and high energy collider physics, depending on whether the doubly charged scalar S appears as a virtual or real particle [20]. However such a model cannot account for DM, since the doubly charged scalar S decays promptly into either pairs of like-sign charged leptons or W bosons. Here we shall extend the model slightly by introducing an additional neutral scalar ϕ and assume an unbroken Z_2 symmetry in the scalar sector, under which only the additional neutral scalar ϕ is odd, which then becomes a stable DM candidate. The model may be regarded as an extension of the so-called Higgs portal scenario [30], in the presence of a doubly charged scalar which accounts for neutrino mass and mixing. The resulting framework presented here, involving both S and ϕ , then merges two apparently unrelated features: the existence of a new physics sector at the TeV scale, providing naturally small neutrino masses, and the existence of a good DM candidate.

The layout of the remainder of the paper is as follows. In section 2 we review the effective model proposed and studied in [19, 20] involving just one extra particle, the doubly charged scalar S . In section 3 we extend this model by introducing an additional neutral scalar ϕ , and discuss the resulting scalar potential of the model involving the Higgs doublet H , the doubly charged scalar S and the neutral scalar ϕ . We then go on to calculate the relic abundance of the DM particles ϕ and their prospects for direct and indirect detection. Section 4 concludes the paper.

2. The effective model with a doubly charged scalar

In this section we review the effective Lagrangian model presented in [19], in which the SM is extended by adding one new scalar particle: a complex $SU(2)_L$ singlet, hypercharge $Y = 2$ (hence electric charge $Q = 2$) state S^{++} and its antiparticle S^{--} , both doubly charged and denoted in the following as S and S^\dagger respectively.

The doubly charged scalar field S has an effective coupling to the SM W^\pm bosons as well as to same-sign right-handed charged SM leptons, giving rise to a rich phenomenology. In addition to contributing to flavour violating leptonic processes, to leptonic dipole moments and to leptonic radiative decays, the scalar S allows a 2-loop diagram which is responsible for providing all mass (and mixings) to neutrinos. It is shown in [19] that the lowest mass dimension at which the vertex SWW can be realised is by effective operators of dimension $d = 7$. The relevant operator, in the unitary gauge, for the generation of neutrino masses is:

$$\mathcal{L}_{SWW} = -\frac{g^2 \xi v^4}{4\Lambda^3} (S W^\mu W_\mu + h.c.) \quad (2.1)$$

being ξ an order $\mathcal{O}(1)$ dimensionless parameter and Λ the new physics scale above which the effective theory breaks. The coupling of S to same-sign RH leptons is given by

$$\mathcal{L}_{Sll} = f_{ab} S^\dagger \bar{l}_a P_L l_b^c + h.c. \quad (2.2)$$

with f_{ab} dimensionless parameters. There are strong experimental constraints on the f_{ab} parameter space, basically due to the flavour violating couplings of the charged scalar S with leptons, the strongest bound proceeding from $\mu \rightarrow e\gamma$ and $\mu \rightarrow 3e$. A detailed analysis of these bounds can be found in [19,20,23].

The simultaneous presence of the SWW and Sll vertices generate a 2-loop contribution to the neutrino masses, that schematically can be written as

$$\mathcal{M}_\nu^{2\text{-loop}} = 2\xi f_{ab}(1 + \delta_{ab}) \frac{m_a m_b m_S^2}{\Lambda^3} \tilde{\mathcal{I}}(m_W, m_S, \mu) \quad (2.3)$$

where m_S is the S particle mass, m_i is the mass of the l_i lepton, δ_{ab} is the Kronecker delta and $\tilde{\mathcal{I}}(m_W, m_S, \mu)$ is the two loop integral calculated in [19].

Apart from the usual contribution to $0\nu\beta\beta$ due to massive neutrinos in presence of a lepton number violating interaction, this model also produce an additional non-standard contribution to it, since the doubly charged scalar S can couple both to W^-W^- and e^-e^- . Taking into account the newest GERDA results of $T_{1/2}^{0\nu\beta\beta}(\text{Ge}) > 2.1 \cdot 10^{25}$ at 90% C.L., [24], one obtains

$$\frac{\xi f_{ee}}{M_S^2 \Lambda^3} < \frac{4.0 \cdot 10^{-3}}{\text{TeV}^5}. \quad (2.4)$$

In general it is not an easy task to fulfil all the flavour/dipole bounds and obtain a realistic description for neutrino masses and mixing compatible with the $0\nu\beta\beta$ decay bounds. In [19] a detailed analysis has been performed that highlighted the presence of three typical regions where this may happen, hereafter denoted as “Benchmark Scenarios”:

1. Benchmark Scenario A: $f_{ee} \simeq 0$ and $f_{e\tau} \simeq 0$. In this region the additional contribution to the $0\nu\beta\beta$ essentially vanishes. A normal hierarchy between the neutrino masses with the lightest one around 5 meV is obtained;
2. Benchmark Scenario B: $f_{ee} \simeq 0$ and $f_{e\mu} \simeq -(f_{\mu\tau}^*/f_{\mu\mu}^*)f_{e\tau}$. In this region one still has a vanishing additional contribution to the $0\nu\beta\beta$ and a normal ordered neutrino masses with the lightest one around 5 meV. However the constraint relating $f_{e\mu}$ and $f_{e\tau}$ makes this scenario more predictive (falsifiable) in what concerns lepton flavour violation;
3. Benchmark Scenario C: $f_{e\mu} \simeq -(f_{\mu\tau}^*/f_{\mu\mu}^*)f_{e\tau}$. In this region one can assume large values for the f_{ee} coupling. However not to enter in conflict with the GERDA limit on $0\nu\beta\beta$ of Eq. (2.4) one has to push the cutoff scale Λ to several TeV, not a desirable thing from the collider phenomenology point of view.

For the analysis presented in the following sections we will use the best fit benchmark point for each of the three scenarios reported by [19]:

1. Benchmark Point A: $m_S = 164.5$ GeV, $\Lambda = 905.9$ GeV, $\xi = 5.02$;
2. Benchmark Point B: $m_S = 364.6$ GeV, $\Lambda = 2505.1$ GeV, $\xi = 6.38$;
3. Benchmark Point C: $m_S = 626.0$ GeV, $\Lambda = 5094.7$ GeV, $\xi = 3.39$.

3. Higgs portal DM with a doubly charged scalar

In order to account for DM, we now introduce a further particle into the scheme of the previous section, namely an electrically neutral real scalar ϕ . An unbroken Z_2 symmetry is assumed, under which the field ϕ is odd, while all the other particles are even. The motivation of such a setup is twofold: firstly, as already discussed, the presence of an extra doubly charged scalar can provide an economical mechanism for triggering light neutrino masses and mixing [19–22]. Secondly, the new neutral scalar can account for DM. Possible UV completions of this model could be pursued along the lines of [21,22]. Here we shall not try to construct an ultraviolet complete model, but continue to consider the effective theory below the cut-off Λ , where the theory has a rather minimal particle content, with the goal of understanding DM in this extended model. In particular, we shall discuss how the presence of an extended scalar sector can potentially modify the limits and the predictions obtained in the standard DM Higgs portal scenario [30]. In

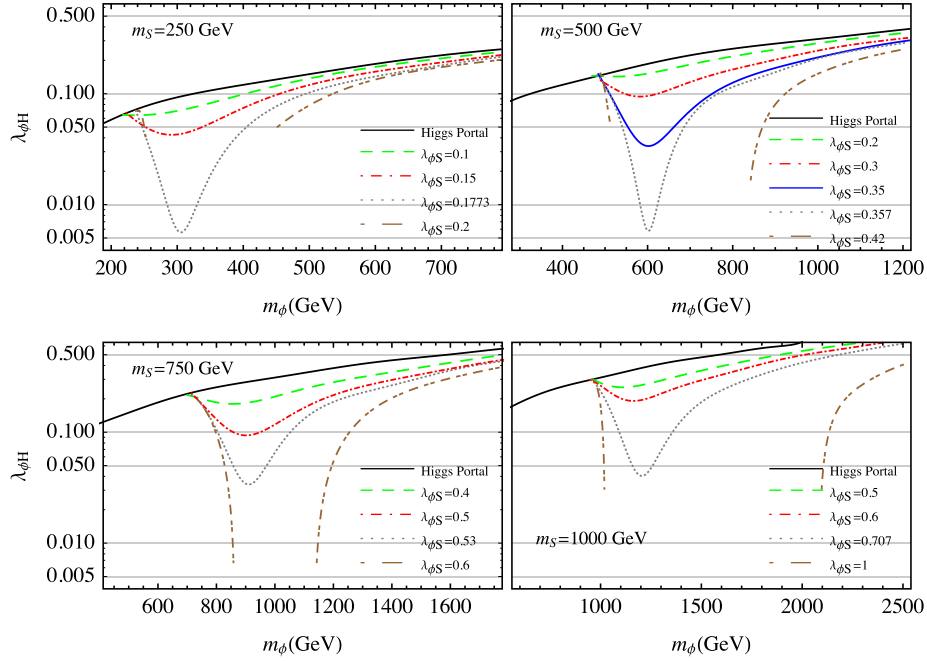


Fig. 1. Allowed parameter space, in the $(m_\phi, \lambda_{\phi H})$ plane, for which the DM relic abundance reproduces the observed value, $\Omega_{DM}h^2 = 0.1198$ [60]. The four plots correspond to four different values of $m_S = 250, 500, 750, 1000$ GeV, respectively. In each plot several choices for $\lambda_{\phi S}$ are shown. (For interpretation of the colours in this figure, the reader is referred to the web version of this article.)

this section we study the DM signatures of the effective Lagrangian model described in the previous section.

The most general (renormalizable) scalar potential for the model at hand is given by

$$\begin{aligned}
 V = & \mu^2 |H^\dagger H| + \lambda |H^\dagger H|^2 + \frac{1}{2} \mu_\phi^2 \phi^2 \\
 & + \frac{1}{4} \lambda_\phi \phi^4 + \mu_S^2 S^\dagger S + \lambda_S (S^\dagger S)^2 + \\
 & + \frac{1}{2} \lambda_{\phi H} \phi^2 |H^\dagger H| + \lambda_{SH} (S^\dagger S) |H^\dagger H| + \frac{1}{2} \lambda_{\phi S} \phi^2 (S^\dagger S) \quad (3.1)
 \end{aligned}$$

where H is the usual SM Higgs doublet, S the doubly charged scalar and ϕ the additional neutral scalar, odd under the unbroken \mathbb{Z}_2 symmetry, that will play eventually the role of stable DM. In addition to the SM Higgs sector parameters, μ and λ , compatibly with the assumption of an unbroken \mathbb{Z}_2 symmetry, one can introduce seven additional dimensionless parameters: a quadratic and a quartic self-interacting couplings, respectively for the neutral and charged exotic scalars, plus three parameters associated to the quartic mixings between all the neutral and charged scalars. We assume that the ElectroWeak Symmetry Breaking (EWSB) is associated exclusively to the Higgs sector, i.e. $\mu^2 < 0$ is assumed while $\mu_\phi^2, \mu_S^2 > 0$ are considered. The masses of the exotic scalars, then, read

$$m_\phi^2 \equiv \mu_\phi^2 + \frac{1}{2} \lambda_{\phi H} v^2, \quad m_S^2 \equiv \mu_S^2 + \frac{1}{2} \lambda_{SH} v^2 \quad (3.2)$$

It is interesting to compare the predictions of this model with the ones of the minimal Higgs portal DM, which is described by the potential of Eq. (3.1) once the doubly charged scalar is decoupled from the theory, i.e. $m_S \gg m_H, m_\phi$ or by setting $\lambda_{\phi S} = 0 = \lambda_{SH}$.¹ The phenomenology of such a minimal Higgs portal DM

model has been extensively studied in [25–38,42–51,56]. Here we are interested in how the presence of the doubly charged scalar can affect Higgs portal DM.

3.1. Relic abundance

In order to obtain the DM relic abundance one has to solve the following Boltzman equation:

$$\frac{dY}{dT} = \sqrt{\frac{\pi g_*(T)}{45}} M_P \langle \sigma v \rangle \left(Y(T)^2 - Y_{eq}(T)^2 \right) \quad (3.3)$$

where $Y(T)$ is the DM abundance, $Y_{eq}(T)$ is the equilibrium thermal abundance, g_* is the effective number of degrees of freedom, M_P is the Planck mass and $\langle \sigma v \rangle$ is the thermally averaged annihilation cross section, which must include all relevant annihilation processes:

$$\langle \sigma v \rangle = \int_{4m_\phi^2}^{\infty} \frac{s \sqrt{s - 4m_\phi^2} K_1(\sqrt{s}/T) \sigma v_{rel}}{16T m_\phi^4 K_2^2(m_\phi/T)} ds \quad (3.4)$$

where K_1 and K_2 are modified Bessel functions of the second kind. The present DM abundance, $Y(T_0)$, is obtained by integrating Eq. (3.3) down to the today temperature T_0 . Then, the DM relic density is

$$\Omega_{DM} h^2 = 2.74 \times 10^8 \frac{m_\phi}{\text{GeV}} Y(T_0). \quad (3.5)$$

We computed these quantities using the publicly available version of micrOMEGAs [57,58].

In Fig. 1 we plot the allowed parameter space in the $(m_\phi, \lambda_{\phi H})$ plane for which the DM relic abundance coincides with the observed value, $\Omega_{DM}h^2 = 0.1198$ [60]. The four plots correspond to four different values of $m_S = 250, 500, 750, 1000$ GeV, respectively. In each plot of Fig. 1, the full black curve represents the Higgs portal case (i.e. $\lambda_{\phi S} = 0 = \lambda_{SH}$). Then, for each plot the dashed,

¹ Notice, however, that the decoupling limit is only approximately reached by setting one of the tree level parameters, for example $\lambda_{\phi S}$, to zero, while keeping the other two finite. In fact in this case one can generate a one-loop contribution to $\lambda_{\phi S}$ through the $\lambda_{\phi H}$ and λ_{SH} vertices. We will come back later on this point.

dot-dashed, dotted and dot-dot-dashed curve are obtained for representative choices of $\lambda_{\phi S}$, which value is shown in the legenda. There is no significant dependence from the chosen value of λ_{SH} , which has been conventionally taken $\lambda_{SH} = 1$.²

When the DM particle, ϕ , is lighter than the doubly charged scalar, S , the process $\phi\phi \rightarrow SS^\dagger$ is not efficient, and the relic abundance results as in the pure Higgs portal case, i.e. via the pair $\phi\phi$ annihilating into an off-shell Higgs scalar mediating the processes $\phi\phi \rightarrow W^+W^-, ZZ, HH, t\bar{t}$ or at tree level into a pair of Higgs scalars. We'll refer collectively to these processes as $\phi\phi \rightarrow SM$.

The same happens when $m_\phi \gg m_S$. However, in the intermediate region, $m_\phi \approx m_S$, the process $\phi\phi \rightarrow SS^\dagger$ becomes efficient and, accordingly, $\lambda_{\phi H}$ needs to be suppressed, depending on the chosen value for $\lambda_{\phi S}$, in order to reproduce the correct amount of DM relic density. In particular, for large enough $\lambda_{\phi S}$ and for specific values of the m_ϕ mass all the relic abundance can be produced exclusively via the coupling $\lambda_{\phi S}$, with $\lambda_{\phi H}$ approaching zero. This is why the dot-dot-dashed (brown) curve exists only in the “small” and “large” m_ϕ region. For such values of $\lambda_{\phi S}$, in the intermediate m_ϕ range, DM is overproduced, and the set of parameter chosen is not allowed. This fact can be clearly seen in the $m_S = 750$ GeV (lower-left) plot: for $\lambda_{\phi S} = 0.6$ and $850 \lesssim m_\phi \lesssim 1150$ GeV one can never reproduce the correct amount of DM density.

A comment is in order regarding the possibility of setting $\lambda_{\phi H} = 0$. In the framework at hand, $\lambda_{\phi H}$ can receive loop contributions, through diagrams involving $\lambda_{\phi S}$ and λ_{SH} couplings. It can be shown that, for a temperature $T > m_\phi/20$, $\langle\sigma v\rangle$ (and therefore $\lambda_{\phi H}$) doesn't have an impact on $Y(T)$, since for those temperatures the DM abundance is equal to the equilibrium abundance, $Y(T) = Y_{eq}(T)$. When $T \sim m_\phi/20$, the DM particle freezes-out, and the relic abundance depends indeed on $\langle\sigma v\rangle$. As a conclusion, the typical energies in which the loop is relevant is when $p^2 \sim (m_\phi/20)^2$. Setting the renormalization scale at $2m_S$, at one loop one obtains:

$$\lambda_{\phi H}^{ren} \simeq \lambda_{\phi H} + \frac{1}{16\pi^2} \lambda_{\phi S} \lambda_{SH} \log \frac{m_\phi}{40m_S} \quad (3.6)$$

As typically the loop contribution is few 10^{-3} , one cannot extrapolate the tree level analysis to values of $\lambda_{\phi H}$ below few 10^{-3} . In plotting our results we always work with $\lambda_{\phi H} \geq 0.005$.

All these comments are clearly summarised in Fig. 2 where the parameter space which yields the correct relic abundance, in the $(\lambda_{\phi S}, \lambda_{\phi H})$ plane, is shown for $m_S = 500$ GeV. The light-red region summarises the region, allowed by relic density data, for the relevant couplings of our DM model. Inside the filled region for definiteness we have also shown few dashed lines for various m_ϕ values. For $m_\phi \leq m_S$ one typically spans the lower-left region of the parameter space, while for $m_\phi \geq m_S$ one spans the upper and the right part of the filled area. In particular, we clearly see the existence of a critical value: $\lambda_{\phi S}^{crit} = 0.357$ for this specific m_S case. For $\lambda_{\phi S} \leq \lambda_{\phi S}^{crit}$ it is always possible to find values for $\lambda_{\phi H}$ and $\lambda_{\phi S}$ in order to satisfy the relic abundance bound, independently of the m_ϕ mass. In fact one always cross all different colours dashed lines. For $\lambda_{\phi S} \geq \lambda_{\phi S}^{crit}$, only for specific ranges of m_ϕ one can find a solution.

It should be noted that the annihilation of two DM particles, ϕ , moving at non-relativistic velocities could be enhanced due to the Sommerfeld effect [39,40]. In our case, this effect can only be mediated by a t-channel Higgs exchange. However, it was shown

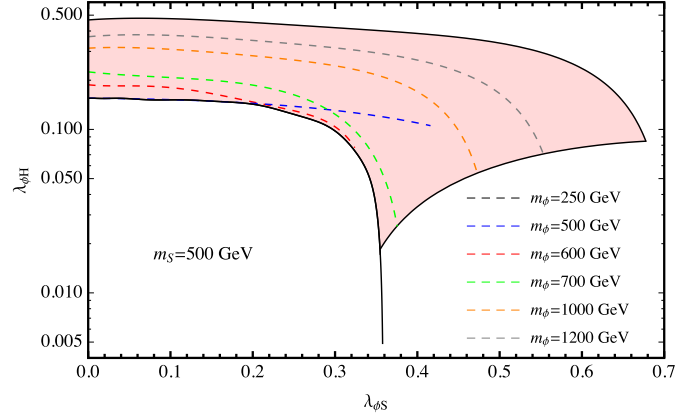


Fig. 2. Allowed parameter space in the $(\lambda_{\phi S}, \lambda_{\phi H})$ plane for $m_S = 500$ GeV and $m_\phi \in (500, 1500)$ GeV. The value for $m_\phi = 250$ GeV is shown in order to illustrate the fact that, for m_ϕ below m_S , the coupling $\lambda_{\phi S}$ has no impact. (For interpretation of the colours in this figure, the reader is referred to the web version of this article.)

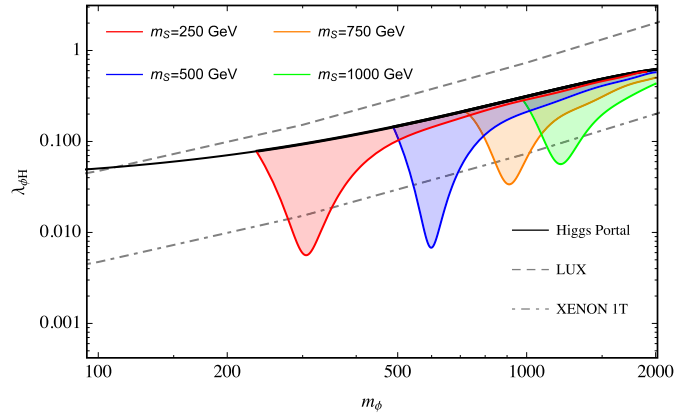


Fig. 3. Allowed parameter space in the $(\lambda_{\phi H}, m_\phi)$ plane for four different m_S values ($m_S = 250, 500, 750, 1000$ GeV). Dashed and dot-dashed black lines represent the exclusion limits from direct detection by LUX and (the prediction for) XENON 1T, respectively.

in [41] that such an enhancement is relevant only for $m_\phi > 2$ TeV, which is outside the range of masses considered in the present analysis.

3.2. Direct detection

Direct detection experiments can significantly constrain the allowed parameter space for DM models. Experiments like LUX [61] and XENON [62,63] can detect the DM particle scattering with the nucleons of the detector material, which in the both cases is Xenon. In our model, as well as in the pure Higgs portal case, this interaction mainly occurs via exchange of a Higgs scalar. The spin-independent cross-section is given by

$$\sigma_{SI} = \frac{f_N^2 \mu^2 m_N^2}{4\pi m_H^4 m_\phi^2} \lambda_{\phi H}^2 \quad (3.7)$$

with m_N the nucleon mass, $\mu = m_\phi m_N / (m_\phi + m_N)$ the DM-nucleon reduced mass and $f_N \sim 0.3 \pm 0.03$ the hadron matrix element [51, 54,55]. In Fig. 3 we show the limits in the plane $(\lambda_{\phi H}, m_\phi)$ from the current constraints of LUX (dashed black line) and the predicted sensitivity of XENON 1T (dot dashed black line). Both the pure Higgs portal and our model can escape the LUX limit. However, while the Higgs portal scenario will be for sure inside the XENON 1T sensitivity region, our model can for all considered values of m_S , ranging from 250 GeV and 1000 GeV, escape the direct

² On the one hand, since the $\phi\phi$ annihilation occurs almost at rest, $m_S > m_H$ in all the considered scenarios, the $H \rightarrow SS^\dagger$ decay is not relevant. On the other hand, the contributions coming from $SS^\dagger \rightarrow H$ are suppressed by a loop factor.

detection (even taking into account the uncertainty of $\mathcal{O}(10\%)$ in the determination of f_N). As explicitly shown in Figs. 1 and 2, the presence of the new coupling $\lambda_{\phi S}$ can allow values for $\lambda_{\phi H}$ below XENON 1T sensitivity. This feature is almost independent from the chosen m_ϕ and m_S values, in the ≈ 1 TeV region.

3.3. Indirect detection

The DM particles in the galaxy can annihilate and yield several indirect signatures, such as positrons, antiprotons and photons. The detection of these cosmic rays is one of the most promising ways to identify DM existence [64–68]. We will focus here in particular in the observed spectrum of positrons and antiprotons. The production rate of these particles at a position \vec{x} with an energy E is usually expressed as [59]

$$Q_a(\vec{x}, E) = \frac{1}{2} \langle \sigma v \rangle \left(\frac{\rho(\vec{x})}{m_\phi} \right)^2 f_a(E) \quad (3.8)$$

where σv is defined in Eq. (3.4), $\rho(\vec{x})$ is the DM density and $f_a(E) = dN_a/dE$ is the energy distribution of the species a produced in a single annihilation event.

The region of diffusion of cosmic rays is represented by a disk of thickness $2L \simeq (2-30)$ kpc and radius $R \simeq 20$ kpc. The galactic disk is modelled as an infinitely thin disk lying in the middle with half-width $h = 100$ pc and radius R . The charged particles, generated from DM annihilation, propagate in a turbulent regime through the strong galactic magnetic field and are deflected by its irregularities. Monte Carlo simulations show that this motion can be described by an energy dependent diffusion term $K(E)$. On top of that, these particles can lose their energy via inverse Compton scattering on interstellar medium, through Coulomb scattering or adiabatically. This energy loss rate is denoted by $b(E)$. Furthermore these particles can be wiped away by galactic convection, with a velocity $V_C \simeq (5-15)$ km/s [67]. Finally, one has also to account for the annihilation rate Γ_{ann} induced by the interaction of the charged particles with ordinary matter in the galactic disk. Taking into account all these effects, the equation that describes the evolution of the energy distribution of charged particles reads:

$$\frac{\partial}{\partial z} (V_C \psi_a) - \nabla \cdot (K(E) \nabla \psi_a) - \frac{\partial}{\partial E} (b(E) \psi_a) - 2h\delta(z) \Gamma_{ann} \psi_a = Q_a(\vec{x}, E) \quad (3.9)$$

where z is the height in cylindrical coordinates adapted to the disk diffusion model, $\psi_a = dn/dE$ is the number density of particles per unit volume and energy. We use the default settings of micrOMEGAS [59] to numerically evaluate the propagation of positrons and antiprotons that originate from DM annihilation.

3.3.1. Positrons

The energy spectrum of positrons originated from DM annihilation is obtained by solving the diffusion-loss equation keeping only the two dominant contributions: space diffusion and energy losses,

$$-\nabla \cdot (K(E) \nabla \psi_{e^+}) - \frac{\partial}{\partial E} (b(E) \psi_{e^+}) = Q_{e^+}(x, E) \quad (3.10)$$

In addition to the e^+ flux from the DM decay, there exists a secondary positron flux from interactions between cosmic rays and nuclei in the interstellar medium. This positron background $\Phi_{e^+}^{bg}$ can be well approximated as [69,70]

$$\Phi_{e^+}^{bg}(E) = \frac{4.5 \cdot 10^{-4} E^{0.7}}{1 + 650E^{2.3} + 1500E^{4.2}} [\text{GeV}^{-1} \text{m}^{-2} \text{s}^{-1} \text{sr}^{-1}] \quad (3.11)$$

In order to have a better understanding of the $\phi\phi$ annihilation rates we plot the relevant branching ratios in Fig. 4 using the micrOMEGAS tool.

In the left column of Fig. 5 we show the positron flux as function of the positron energy, for the three benchmark points mentioned in Section 2. In each of the three left plots, the dashed (orange) line represents the expected background of Eq. (3.11), while the dot-dashed (black) line is the prediction for the Higgs portal case. The (blue and red) continuous lines represent our model expectations for two different choices of parameters, reported in each plot legenda, which give the correct relic abundance.

The Higgs portal prediction is always at least two orders of magnitude below the astrophysical positron background. For the set of parameters defining Benchmark Point A, the expected positron flux almost coincides with the Higgs portal scenario one. This is due to the fact that for such values of m_ϕ and m_S , the $\phi\phi \rightarrow SS^\dagger$ channel is still suppressed compared to the usual $\phi\phi \rightarrow SM$ one. Moreover, for this Benchmark Point the S coupling to electrons and positrons $f_{ee} \approx 0$. For Benchmark Point B (middle left plot) the $\phi\phi \rightarrow SS^\dagger$ channel becomes more effective compared to the $\phi\phi \rightarrow SM$ one, suppressed by the large m_ϕ mass. Still one has $f_{ee} \approx 0$, the dominant S decays being in WW and $e\tau$ (see [19]). This result in a positron flux two or three times higher than in the Higgs Portal scenario. Finally, for Benchmark Point C (lower left plot) the $\phi\phi \rightarrow SS^\dagger$ channel becomes dominant. Moreover, in this case one has sizeable f_{ee} , letting S mostly decays in positrons. In this region of the parameter space, our model positron flux is one order of magnitude higher compared with the standard Higgs Portal scenario, even if still one order below the expected background.

3.3.2. Antiprotons

The propagation of antiprotons originated from DM annihilation, neglecting the energy loss term, can be described as [71]

$$-K_{\bar{p}} \nabla^2 \psi_{\bar{p}} + V_C \frac{\partial}{\partial z} \psi_{\bar{p}} + 2h\delta(z) \Gamma_{ann} \psi_{\bar{p}} = Q_{\bar{p}}(x, E) \quad (3.12)$$

The astrophysical antiproton background $\Phi_{\bar{p}}^{bg}$ can be written as [72]

$$\Phi_{\bar{p}}^{bg} = \frac{0.9E^{-0.9}}{14 + 30E^{-1.85} + 0.08E^{2.3}} [\text{GeV}^{-1} \text{m}^{-2} \text{s}^{-1} \text{sr}^{-1}] \quad (3.13)$$

The plots on the right column of Fig. 5 show that, as in the positron case, the antiproton flux predicted in the Higgs portal scenario (dot-dashed black line) is roughly two orders of magnitude below the astrophysical background (dashed orange curve).

The doubly charged particle has a largest branching fraction to W s in Benchmark Point A than in the rest of cases [19]. Thus, even if in this region of parameter space the $\phi\phi \rightarrow SM$ process still dominates, the flux of antiprotons for $E \leq 200$ GeV is higher than the one predicted in the Higgs Portal case. However, for Benchmark Points B and C, where the S scalar decays mostly to leptons ($e\tau$ and ee , respectively), the increasing relevance of the $\phi\phi \rightarrow SS^\dagger$ process makes the \bar{p} flux smaller than the corresponding Higgs Portal case for the same m_ϕ mass (compare the black and red lines in middle and bottom left plots of Fig. 5, respectively for $m_\phi = 450$ GeV and $m_\phi = 750$ GeV).

In our model one can obtain a larger flux by increasing the ϕ mass. For example for Benchmark Point C (bottom left plot in Fig. 5), one can obtain a rather larger contribution to the antiproton flux selecting $m_\phi = 1000$ GeV, but still one order of magnitude smaller than the expected \bar{p} background.

3.3.3. Photons

The possibility of indirect detection via photons deserves a comment. The continuum spectrum of photons isn't expected to

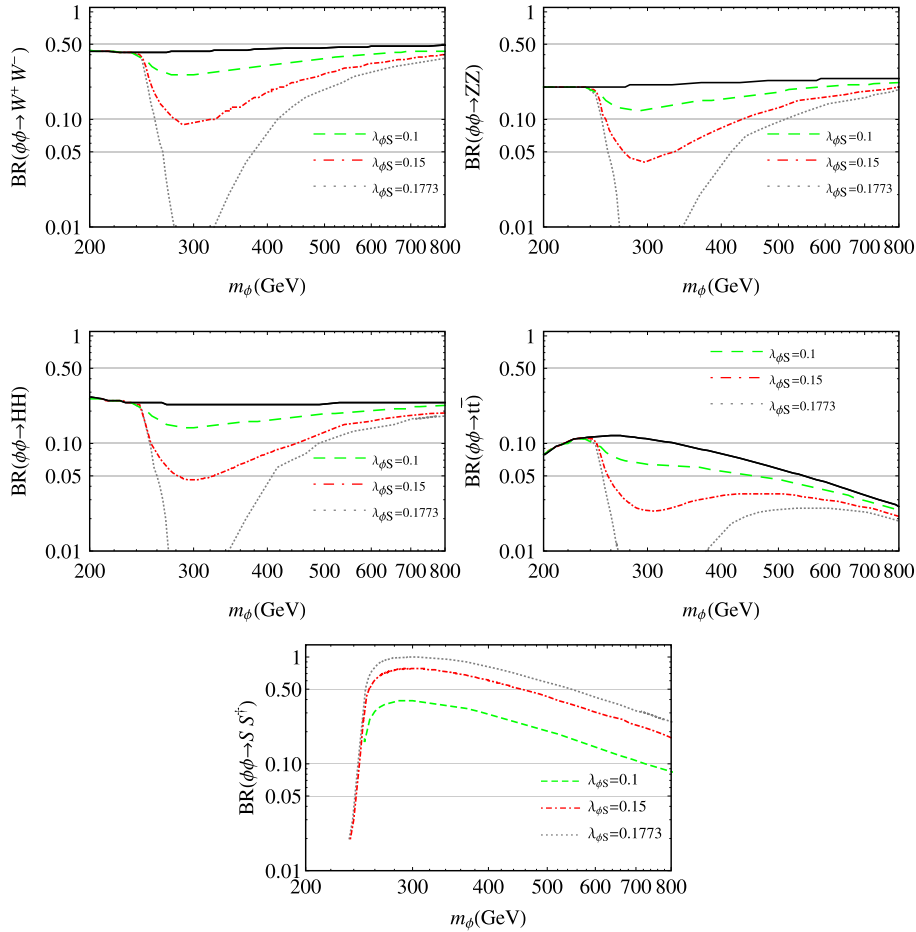


Fig. 4. Branching ratios for $\phi\phi$ to annihilate into various states versus the DM mass with $m_S = 250$ GeV. The value of $\lambda_{\phi H}$ is fixed so that the relic density matches the observed value. In each plot several choices for $\lambda_{\phi S}$ are shown. The black curves correspond to the pure Higgs portal predictions.

change significantly from the Higgs portal scenario, analogously to the positrons and antiprotons case. Therefore, most of the analysis done in [51] would apply as well to our model. Moreover, also the gamma rays excess in the continuum spectrum from the Galactic Centre, claimed by Fermi-LAT, cannot be explained in the Higgs portal scenario [51]. Since the relevant region points at a mass of around 50 GeV, the introduction of an heavy doubly charged S scalar would not significantly change this conclusion.

A more interesting phenomenological aspect would be the production of monochromatic gamma-ray lines and their observation/exclusion by Fermi-LAT experiment. Since the DM candidate is neutral, the production of a monochromatic gamma-ray line must be loop-mediated. The $\phi\phi \rightarrow \gamma\gamma$ annihilation process mediated by a doubly charged S loop has been studied in [52], trying to explain the 130 GeV gamma-ray line [53]. In order to reach the observed sensitivity the author of [52] has to enhance the $\phi\phi \rightarrow \gamma\gamma$ cross section by considering S embedded in a multiplet of an additional $SU(N)$ strong symmetry. This leads to an N_C dependence of the amplitude. For $\lambda_{\phi S} \sim \mathcal{O}(1)$ and $m_S \sim 250$ GeV one needs $N_C \sim 9$ to reach the observed rate. In our scenario we don't have a similar enhancement.

4. Conclusions

In this letter we have considered an extension of the Standard Model involving two new scalar particles around the TeV scale: a singlet neutral scalar ϕ , that plays the role of the Dark Matter

candidate plus a doubly charged $SU(2)_L$ singlet scalar, S^{++} , that is the source for the non-vanishing neutrino masses and mixings. In this framework, besides being able to explain naturally the smallness of neutrino masses with the new physics at the TeV scale, it could be possible to identify DM scenarios which extend the conventional Higgs portal one. We have studied the allowed parameter space for our model, compatible with the present DM relic density. Moreover we have identified possible signatures from direct and indirect DM detection experiments. In general our results indicate that it would be possible, within our framework, to evade XENON 1T exclusion limits for a significant region of the parameter space. However, we also show that, even if the positron and antiproton flux, originating from DM annihilation, is higher than the standard Higgs portal one, it is still about an order of magnitude lower than the observed background.

In conclusion, our model may be regarded as an extension of the minimal Higgs portal DM scenario with a doubly charged scalar which can account for neutrino mass and mixing. The presence of the doubly charged scalar S introduces a new portal coupling of the DM particle ϕ to S , namely $\lambda_{\phi S}$, in addition to the usual Higgs portal coupling of ϕ to the Higgs doublet H , $\lambda_{\phi H}$. The new portal coupling $\lambda_{\phi S}$ becomes important when m_ϕ exceeds m_S , since then it allows the DM particle to annihilate into pairs of doubly charged scalars, as an alternative to the usual DM annihilation into Higgs pairs. This in turn reduces the coupling $\lambda_{\phi H}$, consistent with the desired relic density, making DM harder to detect by direct detection experiments.

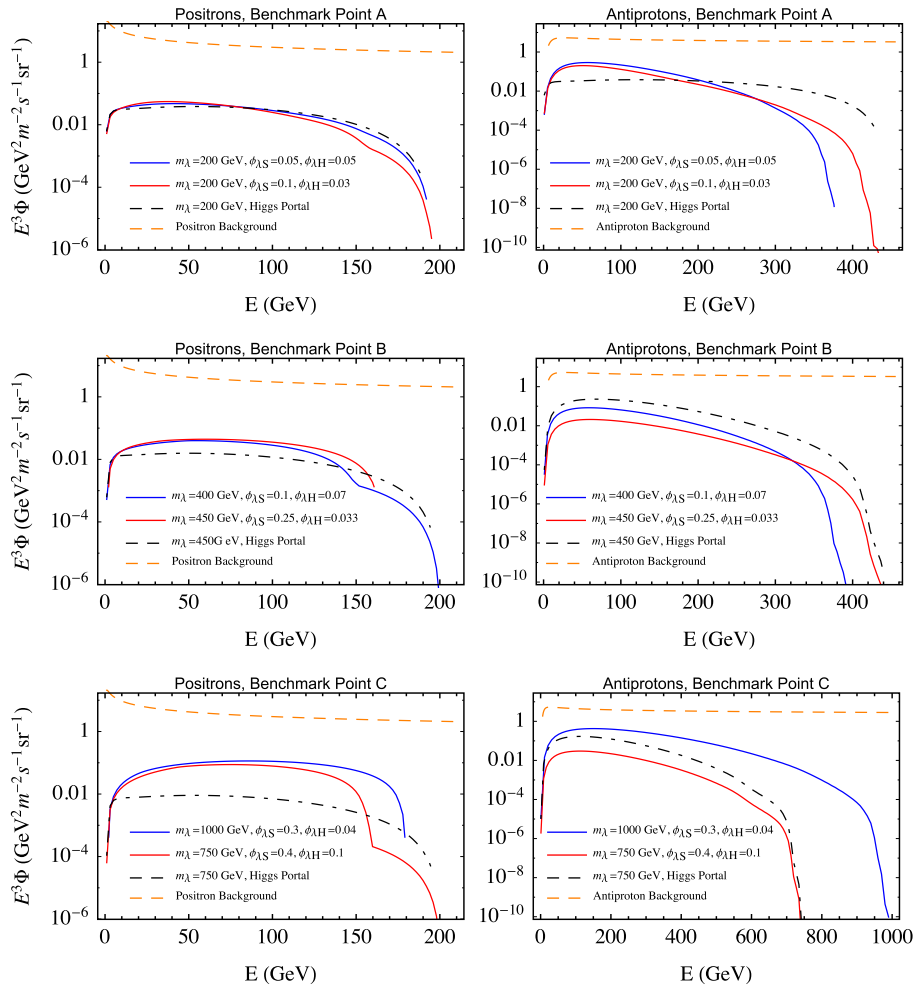


Fig. 5. Predicted positron (left column plots) and antiproton (right column plots) fluxes for the chosen benchmark points A, B and C respectively. (For interpretation of the colours in this figure, the reader is referred to the web version of this article.)

Acknowledgements

The authors acknowledge support from the European Union Horizon 2020 research and innovation programme under the Marie Skłodowska-Curie grant agreements InvisiblesPlus RISE No. 690575, Elusives ITN No. 674896 and Invisibles ITN No. 289442. SFK acknowledge support from the STFC Consolidated grant ST/L000296/1.

References

- [1] G. Aad, et al., ATLAS Collaboration, *Phys. Lett. B* 716 (2012) 1, arXiv:1207.7214 [hep-ex].
- [2] S. Chatrchyan, et al., CMS Collaboration, *Phys. Lett. B* 716 (2012) 30, arXiv:1207.7235 [hep-ex].
- [3] S.F. King, *Rep. Prog. Phys.* 67 (2004) 107, arXiv:hep-ph/0310204; H. Ishimori, T. Kobayashi, H. Ohki, Y. Shimizu, H. Okada, M. Tanimoto, *Prog. Theor. Phys. Suppl.* 183 (2010) 1, arXiv:1003.3552; G. Altarelli, F. Feruglio, *Rev. Mod. Phys.* 82 (2010) 2701, arXiv:1002.0211; S.F. King, A. Merle, S. Morisi, Y. Shimizu, M. Tanimoto, *New J. Phys.* 16 (2014) 045018, arXiv:1402.4271; S.F. King, C. Luhn, *Rep. Prog. Phys.* 76 (2013) 056201, arXiv:1301.1340; S.F. King, *J. Phys. G, Nucl. Part. Phys.* 42 (2015) 123001, arXiv:1510.02091.
- [4] P. Minkowski, *Phys. Lett. B* 67 (1977) 421; M. Gell-Mann, P. Ramond, R. Slansky, in: *Sanibel Talk, CALT-68-709*, Feb 1979, and in *Supergravity*, North-Holland, Amsterdam, 1979; T. Yanagida, in: *Proc. of the Workshop on Unified Theory and Baryon Number of the Universe*, KEK, Japan, 1979; S.L. Glashow, *Cargèse Lect. Phys.* (1979); R.N. Mohapatra, G. Senjanovic, *Phys. Rev. Lett.* 44 (1980) 912; J. Schechter, J.W.F. Valle, *Phys. Rev. D* 22 (1980) 2227.
- [5] M. Hirsch, M.A. Diaz, W. Porod, J.C. Romao, J.W.F. Valle, *Phys. Rev. D* 62 (2000) 113008, arXiv:hep-ph/0004115; M. Hirsch, M.A. Diaz, W. Porod, J.C. Romao, J.W.F. Valle, *Phys. Rev. D* 65 (2002) 119901, Erratum.
- [6] M. Magg, C. Wetterich, *Phys. Lett. B* 94 (1980) 61.
- [7] J. Schechter, J.W.F. Valle, *Phys. Rev. D* 22 (1980) 2227.
- [8] G. Lazarides, Q. Shafi, C. Wetterich, *Nucl. Phys. B* 181 (1981) 287.
- [9] E. Ma, *Phys. Rev. D* 73 (2006) 077301, arXiv:hep-ph/0601225.
- [10] A. Zee, *Nucl. Phys. B* 264 (1986) 99.
- [11] K.S. Babu, *Phys. Lett. B* 203 (1988) 132.
- [12] A. Bandyopadhyay, et al., ISS Physics Working Group Collaboration, *Rep. Prog. Phys.* 72 (2009) 106201, arXiv:0710.4947 [hep-ph].
- [13] S.S.C. Law, K.L. McDonald, *Int. J. Mod. Phys. A* 29 (2014) 1450064, arXiv:1303.6384 [hep-ph].
- [14] P.W. Angel, N.L. Rodd, R.R. Volkas, *Phys. Rev. D* 87 (7) (2013) 073007, arXiv:1212.6111 [hep-ph].
- [15] K.S. Babu, C.N. Leung, *Nucl. Phys. B* 619 (2001) 667, arXiv:hep-ph/0106054.
- [16] F. Bonnet, M. Hirsch, T. Ota, W. Winter, *J. High Energy Phys.* 1303 (2013) 055, arXiv:1212.3045 [hep-ph]; F. Bonnet, M. Hirsch, T. Ota, W. Winter, *J. High Energy Phys.* 1404 (2014) 090, Erratum.
- [17] P. Fileviez Perez, T. Han, G.y. Huang, T. Li, K. Wang, *Phys. Rev. D* 78 (2008) 015018, arXiv:0805.3536 [hep-ph].
- [18] E.J. Chun, P. Sharma, *Phys. Lett. B* 728 (2014) 256, arXiv:1309.6888 [hep-ph].
- [19] S.F. King, A. Merle, L. Panizzi, *J. High Energy Phys.* 1411 (2014) 124, arXiv:1406.4137 [hep-ph].
- [20] T. Geib, S.F. King, A. Merle, J.M. No, L. Panizzi, *Phys. Rev. D* 93 (7) (2016) 073007, arXiv:1512.04391 [hep-ph].
- [21] M. Gustafsson, J.M. No, M.A. Rivera, *Phys. Rev. Lett.* 110 (21) (2013) 211802, arXiv:1212.4806 [hep-ph];

- M. Gustafsson, J.M. No, M.A. Rivera, Phys. Rev. Lett. 112 (25) (2014) 259902, Erratum.
- [22] K.S. Babu, C. Macesanu, Phys. Rev. D 67 (2003) 073010, arXiv:hep-ph/0212058.
- [23] J. Herrero-García, M. Nebot, N. Rius, A. Santamaria, Nucl. Phys. B 885 (2014) 542, arXiv:1402.4491 [hep-ph].
- [24] M. Agostini, et al., GERDA Collaboration, Phys. Rev. Lett. 111 (12) (2013) 122503, <http://dx.doi.org/10.1103/PhysRevLett.111.122503>, arXiv:1307.4720 [nucl-ex].
- [25] V. Silveira, A. Zee, Phys. Lett. B 161 (1985) 136.
- [26] J. McDonald, Phys. Rev. D 50 (1994) 3637, arXiv:hep-ph/0702143.
- [27] C.P. Burgess, M. Pospelov, T. ter Veldhuis, Nucl. Phys. B 619 (2001) 709, arXiv:hep-ph/0011335.
- [28] H. Davoudiasl, R. Kitano, T. Li, H. Murayama, Phys. Lett. B 609 (2005) 117, arXiv:hep-ph/0405097.
- [29] S.W. Ham, Y.S. Jeong, S.K. Oh, J. Phys. G 31 (2005) 857, arXiv:hep-ph/0411352.
- [30] B. Patt, F. Wilczek, arXiv:hep-ph/0605188.
- [31] D. O'Connell, M.J. Ramsey-Musolf, M.B. Wise, Phys. Rev. D 75 (2007) 037701, arXiv:hep-ph/0611014.
- [32] X.G. He, T. Li, X.Q. Li, H.C. Tsai, Mod. Phys. Lett. A 22 (2007) 2121, arXiv:hep-ph/0701156.
- [33] S. Profumo, M.J. Ramsey-Musolf, G. Shaughnessy, J. High Energy Phys. 0708 (2007) 010, arXiv:0705.2425 [hep-ph].
- [34] V. Barger, P. Langacker, M. McCaskey, M.J. Ramsey-Musolf, G. Shaughnessy, Phys. Rev. D 77 (2008) 035005, arXiv:0706.4311 [hep-ph].
- [35] X.G. He, T. Li, X.Q. Li, J. Tandean, H.C. Tsai, Phys. Rev. D 79 (2009) 023521, arXiv:0811.0658 [hep-ph].
- [36] E. Ponton, L. Randall, J. High Energy Phys. 0904 (2009) 080, arXiv:0811.1029 [hep-ph].
- [37] R.N. Lerner, J. McDonald, Phys. Rev. D 80 (2009) 123507, arXiv:0909.0520 [hep-ph].
- [38] M. Farina, D. Pappadopulo, A. Strumia, Phys. Lett. B 688 (2010) 329, arXiv:0912.5038 [hep-ph].
- [39] J. Hisano, S. Matsumoto, M. Nagai, O. Saito, M. Senami, Phys. Lett. B 646 (2007) 34, <http://dx.doi.org/10.1016/j.physletb.2007.01.012>, arXiv:hep-ph/0610249.
- [40] J.L. Feng, M. Kaplinghat, H.B. Yu, Phys. Rev. D 82 (2010) 083525, <http://dx.doi.org/10.1103/PhysRevD.82.083525>, arXiv:1005.4678 [hep-ph].
- [41] H. Han, S. Zheng, Nucl. Phys. B 914 (2017) 248, <http://dx.doi.org/10.1016/j.nuclphysb.2016.11.015>, arXiv:1510.06165 [hep-ph].
- [42] A. Bandyopadhyay, S. Chakraborty, A. Ghosal, D. Majumdar, J. High Energy Phys. 1011 (2010) 065, arXiv:1003.0809 [hep-ph].
- [43] V. Barger, Y. Gao, M. McCaskey, G. Shaughnessy, Phys. Rev. D 82 (2010) 095011, arXiv:1008.1796 [hep-ph].
- [44] W.L. Guo, Y.L. Wu, J. High Energy Phys. 1010 (2010) 083, arXiv:1006.2518 [hep-ph].
- [45] J.R. Espinosa, T. Konstandin, F. Riva, Nucl. Phys. B 854 (2012) 592, arXiv:1107.5441 [hep-ph].
- [46] S. Profumo, L. Ubaldi, C. Wainwright, Phys. Rev. D 82 (2010) 123514, arXiv:1009.5377 [hep-ph].
- [47] A. Djouadi, A. Falkowski, Y. Mambrini, J. Quevillon, Eur. Phys. J. C 73 (6) (2013) 2455, arXiv:1205.3169 [hep-ph].
- [48] Y. Mambrini, M.H.G. Tytgat, G. Zaharijas, B. Zaldivar, J. Cosmol. Astropart. Phys. 1211 (2012) 038, arXiv:1206.2352 [hep-ph].
- [49] A. Drozd, B. Grzadkowski, J. Wudka, J. High Energy Phys. 1204 (2012) 006, arXiv:1112.2582 [hep-ph]; A. Drozd, B. Grzadkowski, J. Wudka, J. High Energy Phys. 1411 (2014) 130, Erratum.
- [50] B. Grzadkowski, J. Wudka, Phys. Rev. Lett. 103 (2009) 091802, arXiv:0902.0628 [hep-ph].
- [51] J.M. Cline, K. Kainulainen, P. Scott, C. Weniger, Phys. Rev. D 88 (2013) 055025, arXiv:1306.4710 [hep-ph]; J.M. Cline, K. Kainulainen, P. Scott, C. Weniger, Phys. Rev. D 92 (3) (2015) 039906, Erratum.
- [52] J.M. Cline, Phys. Rev. D 86 (2012) 015016, <http://dx.doi.org/10.1103/PhysRevD.86.015016>, arXiv:1205.2688 [hep-ph].
- [53] W.B. Atwood, et al., Fermi-LAT Collaboration, Astrophys. J. 697 (2009) 1071, <http://dx.doi.org/10.1088/0004-637X/697/2/1071>, arXiv:0902.1089 [astro-ph.IM].
- [54] J.M. Alarcon, J. Martin Camalich, J.A. Oller, Phys. Rev. D 85 (2012) 051503, arXiv:1110.3797 [hep-ph].
- [55] J.M. Alarcon, L.S. Geng, J. Martin Camalich, J.A. Oller, Phys. Lett. B 730 (2014) 342, arXiv:1209.2870 [hep-ph].
- [56] F.S. Queiroz, K. Sinha, A. Strumia, Phys. Rev. D 91 (3) (2015) 035006, arXiv:1409.6301 [hep-ph].
- [57] G. Belanger, F. Boudjema, A. Pukhov, A. Semenov, Comput. Phys. Commun. 174 (2006) 577, arXiv:hep-ph/0405253.
- [58] G. Belanger, F. Boudjema, A. Pukhov, A. Semenov, Comput. Phys. Commun. 176 (2007) 367, arXiv:hep-ph/0607059.
- [59] G. Belanger, F. Boudjema, P. Brun, A. Pukhov, S. Rosier-Lees, P. Salati, A. Semenov, Comput. Phys. Commun. 182 (2011) 842, arXiv:1004.1092 [hep-ph].
- [60] P.A.R. Ade, et al., Planck Collaboration, arXiv:1502.01589 [astro-ph.CO].
- [61] D.S. Akerib, et al., LUX Collaboration, Phys. Rev. Lett. 112 (2014) 091303, arXiv:1310.8214 [astro-ph.CO].
- [62] E. Aprile, et al., XENON100 Collaboration, Phys. Rev. Lett. 109 (2012) 181301, arXiv:1207.5988 [astro-ph.CO].
- [63] E. Aprile, et al., XENON Collaboration, J. Cosmol. Astropart. Phys. 1604 (04) (2016) 027, arXiv:1512.07501 [physics.ins-det].
- [64] P. Salati, F. Donato, N. Fornengo, in: G. Bertone (Ed.), Particle dark matter, 2010, pp. 521–546, arXiv:1003.4124 [astro-ph.HE].
- [65] T.A. Porter, R.P. Johnson, P.W. Graham, Annu. Rev. Astron. Astrophys. 49 (2011) 155, arXiv:1104.2836 [astro-ph.HE].
- [66] C.E. Yaguna, J. Cosmol. Astropart. Phys. 0903 (2009) 003, arXiv:0810.4267 [hep-ph].
- [67] A. Goudelis, Y. Mambrini, C. Yaguna, J. Cosmol. Astropart. Phys. 0912 (2009) 008, arXiv:0909.2799 [hep-ph].
- [68] C. Arina, M.H.G. Tytgat, J. Cosmol. Astropart. Phys. 1101 (2011) 011, arXiv:1007.2765 [astro-ph.CO].
- [69] A.W. Strong, I.V. Moskalenko, O. Reimer, Astrophys. J. 613 (2004) 962, arXiv:astro-ph/0406254.
- [70] E.A. Baltz, J. Edsjo, Phys. Rev. D 59 (1998) 023511, arXiv:astro-ph/9808243.
- [71] Q.H. Cao, C.R. Chen, T. Gong, arXiv:1409.7317 [hep-ph].
- [72] E. Nezri, M.H.G. Tytgat, G. Vertongen, J. Cosmol. Astropart. Phys. 0904 (2009) 014, arXiv:0901.2556 [hep-ph].